*Anal. Chem.* **2002,** *74,* 4919−4926

# Numerical Solution of a Multi-Ion One-Potential Model for Electroosmotic Flow in Two-Dimensional Rectangular Microchannels

Achim Van Theemsche,* Johan Deconinck, Bart Van den Bossche, and Leslie Bortels

*Vrije Universiteit Brussel, Pleinlaan 2, 1050 Brussels, Belgium*

**A new more general numerical model for the simulation of electrokinetic flow in rectangular microchannels is presented. The model is based on the dilute solution model and the Navier−Stokes equations and has been implemented in a finite-element-based C++ code. The model includes the ion distribution in the Helmholtz double layer and considers only one single electrical potential field variable throughout the domain. On a charged surface(s) the surface charge density, which is proportional to the local electrical field, is imposed. The $\zeta$ potential results, then, from this boundary condition and depends on concentrations, temperature, ion valence, molecular diffusion coefficients, and geometric conditions. Validation cases show that the model predicts accurately known analytical results, also for geometries having dimensions comparable to the Debye length. As a final study, the electro-osmotic flow in a controlled cross channel is investigated.**

The use of microchannels, initially conceived for biological analysis[1] in the early 1990s, has all the benefits of miniaturization. The time and the cost of performing a series of analyses are reduced by several orders of magnitude and new applications become possible. Apart from biological analysis, the areas that benefit from this modern technology are chemical analysis, environmental analysis, material analysis, measurements in outer space, etc. In the past decade, two major applications of this new technology have been developed: the lab-on-a-chip or micrototal analysis systems ($\mu$TAS) and the microelectromechanical systems (MEMS). The development of $\mu$TAS has progressed in line with the original ideas to use them, for example, for biological labs on a microscale to perform analysis, and is popular in medical industries and biogenetics. MEMS have been specialized for making microvalves, pumps and other mechanical applications, which are used in chemical analysis, and microdevices for all kinds of purposes (industrial, electrodomestic, computers, etc.). In all of these applications, an exact control and understanding of the fluid flow is essential. One of the most interesting techniques to control the fluid movements is based on electroosmotic flow (EOF) or on a combination of a pressure-driven flow with EOF. The numerical solution of the Navier−Stokes (NS) equations, including the local Lorentz force distribution, results in the flow field. This article proposes a one-potential model for the EOF, including the distributions in the Helmholtz double layer (HDL). This model has been implemented in a finite element (FE) solver, and numerical simulations are presented as validation cases. Three geometries are studied: a charged wall, a straight channel, and a cross channel.

Reuss[2] made the first discoveries on EOF. It was but 70 years later that Helmholtz proposed his theory of the HDL.[3] Von Smoluchowski[4] found the well-known relationship between the zeta ($\zeta$) potential in a capillary and the velocity for capillaries with radius, $r$, much larger than the Debye-length, $\lambda$. It is generally accepted that for certain conditions, the EOF can be characterized by a simple channel flow with no-slip boundary conditions, namely the Smoluchowski velocity. Cummings et al.[5] formulated these conditions in his ideal electroosmosis concept and called it "the similitude principle". Many other authors have published on the analytical formulation for EOF.[6−10] Analytical expressions for the velocity were also found for capillaries[7,8,10−12] and two-dimensional channels.[6,9] Thormann et al.[24] proposed analytical formulations of the EOF mobility with respect to the ionic strength.

* Corresponding author. E-mail: avtheems@vub.ac.be.

(1) Harrison, D. J.; Manz, A.; Fan, Z. H.; Ludi, H.; Widmar, H. M. *Anal. Chem.* **1992**, *64*, 1926−1832.
(2) Reuss, F. F. *Memoires de la Societe Imperiale de Naturalistes de Moscou* **1809**, *2*, 327.
(3) Helmholtz, H. *Ann. Phys.* **1879**, *7*, 337.
(4) Smoluchowski, M. *Krak. Anz.* **1903**, 182.
(5) Cummings, E. B.; Griffiths, S. K.; Nilson, R. H.; Paul, P. H. *Anal. Chem.* **2000**, *72*, 2526−2532.
(6) Burgreen, D.; Nakache, F. R. *J. Phys. Chem.* **1964**, *68* (5), 1084−1091.
(7) Rice, C. L.; Whitehead, R. *J. Phys. Chem.* **1965**, *69* (11), 4017−4024.
(8) Keh, H. J.; Liu, Y. C. *J. Colloid Interface Sci.* **1995**, *172*, 222−229.
(9) Bianchi, F.; Wagner, F.; Hoffmann, P.; Girault, H. H. *Anal. Chem.* **2001**, *73*, 829−836.
(10) Dutta, P.; Beskok, A. *Anal. Chem.* **2001**, *73*, 1979−1986.
(11) Probstein, R. F. *Physicochemical Hydrodynamics*; Butterworth Publishers: Boston, 1989.
(12) Newman, J. S. *Electrochemical Systems*; Prentice Hall: Englewood, NJ, 1991.
(13) Patankar, N. A.; Hu, H. H. *Anal. Chem.* **1998**, *70*, 1870−1881.
(14) Ermakov, S. V.; Jacobson, S. C.; Ramsey, J. M. *Anal. Chem.* **1998**, *70*, 4494−4504.
(15) Hu, L.; Harrison, J. D.; Masliyah, J. H. *J. Colloid Interface Sci.* **1999**, *215*, 300−312.
(16) Mitchell, M. J.; Qiao, R.; Aluru, N. R. *J. Microelectromech. Syst.* **2000**, *9* (4), 435−449.
(17) Bortels, L.; Deconinck, J.; Van Den Bossche, B. *J. Electroanal. Chem.* **1996**, *404*, 15−26.
(18) Borukhov, I.; Andelman, D.; Orland, H. *Electrochim. Acta* **2000**, *46* (2−3), 221−229.
(19) Attard, P.; Antelmi, D.; Larson, I. *Langmuir* **2000**, *16*, 1542−1552.

10.1021/ac025609s CCC: $22.00 
Published on Web 08/23/2002

A number of papers have dealt with the numerical modeling of EOF.[13−16] Patankar and Hu[13] modeled EOF in a cross channel. They applied the superposition of two potential distributions, and since then, nearly all of the other authors have used this idea. First, the linearized Poisson−Boltzmann (LPB) equation is solved numerically in order to obtain the charge distributions along the walls. Then the external electric field, inducing the Lorentz force, is obtained by solving a Laplace equation with a properly imposed potential difference. Ermakov et al.[14] used the analytical formulation for the EOF velocity and imposed this velocity as a nonslip boundary condition to solve the incompressible NS equations. They also included chemical reactions, because the $\zeta$ potential is known to be pH-dependent. Hu et al.[15] proposed a model based on the same approach as Patankar and Hu but using the exact Poisson−Boltzmann (PB) equation. Mitchell[16] solved that same model but applied the so-called "finite cloud algorithm". The decoupled potential approach is not valid, however, in geometries with characteristic dimensions that are comparable to the Debye length. Hence, decoupling does not allow modeling of nanoscale applications.

In what follows, the solution of a more general multi-ion model (MIM) is presented. It is the combined numerical solution of the ion concentration fields, the single potential field, the flow field, and the pressure field.

To obtain the flux of each ion, the so-called dilute solution model (DSM)[12] is applied without any simplification. This means that the flux is simultaneously due to convection, migration, and diffusion. The potential field is governed by charge distribution (PB equation). The NS-equations, which include a Lorentz force term, describe the velocity and pressure of the solvent. Note that there is only one flow field (no multiphase flow), but that it need not necessarily be an nonrotational flow. Since the ion concentrations are a direct result of the DSM, it is also applicable for $n$ ions each, with their respective valence.

The models taking into account the effects of the finite ion size are beyond the scope of this work. According to Attard[19] this restriction implies only a rather small error of the $\zeta$ potential.

## THE MULTI-ION MODEL

**Dilute Solution Model.** A solution of ions placed in an electrically isolated environment is electrically neutral everywhere in the solution. The charge conservation law is valid for all species k with concentration $c_k$ and valence $z_k$, yielding

$$\sum_k c_k z_k = 0 \tag{1}$$

If a solution of ions is in contact with a charged surface, the ions close to that surface migrate, and electroneutrality is no longer valid. The zone where the net local charge density is not zero is called the HDL. In the HDL, the amount of electric charge equals the charge on the wall. The ions touching the wall compose the Stern Layer, the ions further from the wall form the diffuse layer, and both layers together are called the HDL. Figure 1 shows schematically the different layers in a solution in contact with a positively charged wall. The $\zeta$ potential is the potential immediately outside the Stern layer. In this work, the finite size of the ions is not incorporated; hence, the $\zeta$ potential is defined as the potential at the charged wall. In the solution, the PB equation couples the ions' distribution with the potential field,

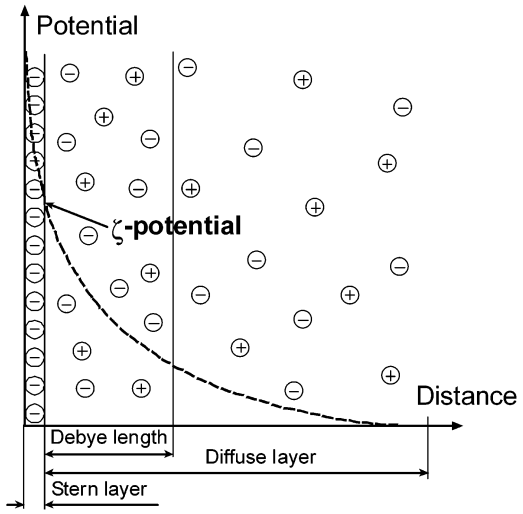


Figure 1. Definitions of Stern layer, Debye length, diffuse layer, and $\zeta$ potential. ⊖, positive ion; ⊕, negative ion and potential distribution.

$$\bar{\nabla}^2 U = -\frac{F}{\epsilon}\sum_k z_k c_k \tag{2}$$

with $U$, the potential (V); $F$, the Faraday constant (96485 C mol$^{-1}$); and $\epsilon$, the permittivity (C V$^{-1}$ m$^{-1}$).

Assuming that the flow is dominated by the solvent and in the absence of homogeneous reactions, the flux $\bar{N}_k$ of each ion k in the solution is given by

$$\bar{N}_k = \bar{v}c_k - z_k u_k F c_k \bar{\nabla}U - D_k \bar{\nabla}c_k \tag{3}$$

Equation 3 expresses that the flux is due to convection of the solvent, migration, and diffusion. The fluid flow velocity is $\bar{v}$ in m s$^{-1}$, $u_k$ represents the ion-mobility (m$^2$ J$^{-1}$ s$^{-1}$), and $D_k$ is the molecular diffusion constant (m$^2$ s$^{-1}$).

For a multi-ion system without the presence of homogeneous reactions, the DSM follows from expressing mass conservation. On the basis of eq 3, this results in

$$\frac{\partial c_k}{\partial t} = -\bar{\nabla}\bar{N}_k = -\bar{\nabla}(\bar{v}c_k) + z_k u_k F \bar{\nabla}(c_k \bar{\nabla}U) + D_k \bar{\nabla}^2 c_k \tag{4}$$

Equations 2 and 4 form the DSM.

Applied to two-dimensional EOF, there exist different relevant boundary (condition) types: inlet, outlet, charged surface, insula-

(20) Zienkiewicz, O. C. *The Finite Element Method in engineering Science*; McGraw-Hill: London, 1971.
(21) Nelissen, G.; Vankeirsbilck, P. F. *Modern Software Tools For Scientific Computing*; Birkhäuser: Boston, 1997; Chapter 4, pp 81−104.
(22) Van der Weide, E. Ph.D. Thesis, TU Delft, Delft, 1998.
(23) Majewski, J.; Athanasiadis, A. N.; Deconinck, H. *Proc. VKI Lecture Series on CFD*; Sint-Genesius-Rode, March 2000.
(24) Thormann, W.; Zhang, C.; Caslavska, J.; Gebauer, P.; Mosher, R. A. *Anal. Chem.* **1998**, *70*, 549−562.

tor, reacting surface, or symmetry axis. For an inlet and outlet, the potential $U$ and the species concentrations $c_k$ are imposed. On a charged surface, the normal electric field is related to the surface charge density distribution.

$$\frac{\partial U}{\partial n} = -\bar{E}\bar{1}_n = -\frac{\sigma}{\epsilon} \tag{5}$$

This boundary condition is imposed on the charged surface for the PB equation. For reacting surfaces (which will not be considered now), one could impose,for example, a Butler−Volmer-type relation[12] between the overpotential at the surface and the flux of each reacting ion. The fluxes of all species are 0 along a symmetry axis or an insulator.

Although the DSM does not take into account the finite ion dimensions or the Stern layer, it contains the influence of the convection on the diffuse layer, an effect that is for EOF by no means negligible. As a consequence, the model remains reliable even for relatively small (compared to $\lambda$) geometries. The potential $U$ found at the surface is considered to be the $\zeta$ potential (Figure 1).

**Incompressible Navier−Stokes.** When Newton's second law is applied to an incompressible Newtonian liquid (solvent), the total variation of the velocity in time of an infinitesimal flow particle is due to pressure gradients, viscous forces, and in the case of EOF, also to Lorentz forces. Together with conservation of mass, the pressure and velocity field can be described by the following incompressible NS equations:[22]

$$\frac{\partial \bar{v}}{\partial t} + (\bar{v}\,\bar{\nabla})\bar{v} = -\frac{\bar{\nabla}_p}{\rho} + \frac{\mu_h}{\rho}\Delta\bar{v} + \frac{\rho_e}{\rho}\bar{\nabla}U \tag{6}$$

$$\bar{\nabla}\cdot\bar{v} = 0 \tag{7}$$

with volumetric charge density (C m$^{-3}$).

$$\rho_e = F\left(\sum_k z_k c_k\right) \tag{8}$$

$p$ is the pressure (Pa); $\rho$, the density (kg m$^{-3}$); and $\mu_h$, the hydraulic diffusion (m$^2$ s$^{-1}$).

The calculation of the force term $\rho_e/\rho\bar{\nabla}U$ is quite different from previously proposed models. In the present approach, this term follows directly from the electric field and the charge distribution obtained from the DSM. The proposed model solves EOF for a single electric potential variable. If one considers, for example, a channel, then the axial potential difference will induce a fluid flow in the axial direction, and the electric field normal to the charged surfaces will have its influence on the pressure distribution in the radial direction, as described by Probstein.[11] Boundary conditions for the NS equations are 0 velocities on the walls, including the charged surfaces, and an imposed pressure on inlets and outlets, although one could also impose a given velocity field along the inlet.

The proposed model could also be applied in three dimensions regardless of the geometry or ion systems considered. The possibility to impose charge densities at the charged surface makes it possible to really calculate the $\zeta$ potential distribution.

## FINITE ELEMENT METHOD

Omitting time dependence, the set of eqs 2, 4, 6, and 7 is solved simultaneously using a FE−Gallerkin discretisation technique.[20] The geometry is subdivided into an unstructured grid of triangular elements in which the unknowns ($c_k$, $U$, $v_x$, $v_y$, and $p$) are supposed to vary linearly. The EOF equations described above have been implemented for steady-state conditions in a code, written in C++ by Nelissen and Vankeirsbilck.[21]

The convective part of the ion flux eq 4 is discretized using a Lax−Wendroff scheme,[22] whereas the diffusion and migration parts are discretized using the standard FE−Gallerkin method. To solve the NS equations, the convective term of eq 6 together with eq 7 are also put in a Lax−Wendroff scheme, and the other terms in the right-hand side of eq 6 are treated in the standard FE−Gallerkin way. The DSM and the NS equations are weakly coupled. This means that, in an iterative way, first eqs 2 and 4 are solved such that a charge distribution and the electric field are found, enabling calculation of the Lorentz forces, after which the flow and pressure fields are calculated by solving eqs 6 and 7. This is repeated until convergence is obtained.

To model properly the evolution of all unknowns, a high-performance hybrid grid generator is used.[23] First, a layered structured grid is generated along all boundaries with a minimal perpendicular element dimension of 0.1 nm adjacent to the surface that grows out with a factor 1.5, up to a total element dimension of 50 nm. Then the remaining part of the geometry is filled in an unstructured way (Delaunay).[23]

## VALIDATION CASES

All subsequent examples will be limited to binary electrolytes in order to enable validation with published data. In the following text, time dependence also will not be considered.

**$\zeta$ Potential of a Charged Surface.** The first validation case considers a dilute solution of a binary electrolyte with 0 velocities near a charged surface. If no fluid flow occurs ($\bar{v} = 0$), the mass conservation of species k is described simply as the equilibrium between diffusion and migration:[17]

$$\frac{\partial c_k}{\partial t} = -\bar{\nabla}\bar{N}_k = z_k u_k F\bar{\nabla}(c_k\bar{\nabla}U) + D_k\bar{\nabla}^2 c_k = 0 \tag{9}$$

The density profile of each ion k normal to the surface is then equal to[11,12]

$$c_k = c_{k0}e^{-z_k FU/RT} \tag{10}$$

and for a binary electrolyte with valences ±1, one can easily substitute the concentrations and deduce the analytical expression for the potential distribution.

$$\Delta U = -\frac{2F}{\epsilon}c_0 \sinh\left(\frac{FU}{RT}\right) \tag{11}$$

Here, the set of eqs 2 and 4 is solved numerically for two ions in a rectangular domain with the boundary conditions as shown in Figure 2. At the nonconducting surface with charge density $\sigma$ in an environment with permittivity $\epsilon$, the electric field is imposed for the PB equation. The ion fluxes normal to the charged surface are put equal to 0. At the boundary far away from the charged surface, which means at least 10 times the Debye length, $\lambda$, the reference potential 0 V is imposed for the PB equation, and the

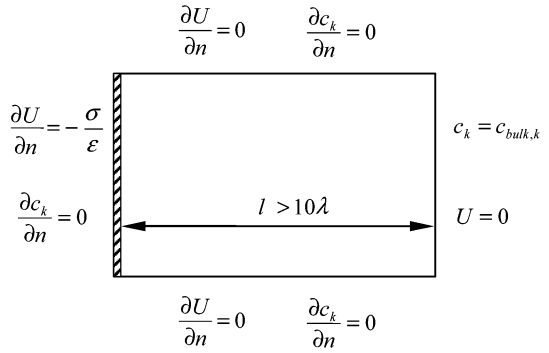


Figure 2. Boundary conditions applied to the simulation of a steady-state HDL.

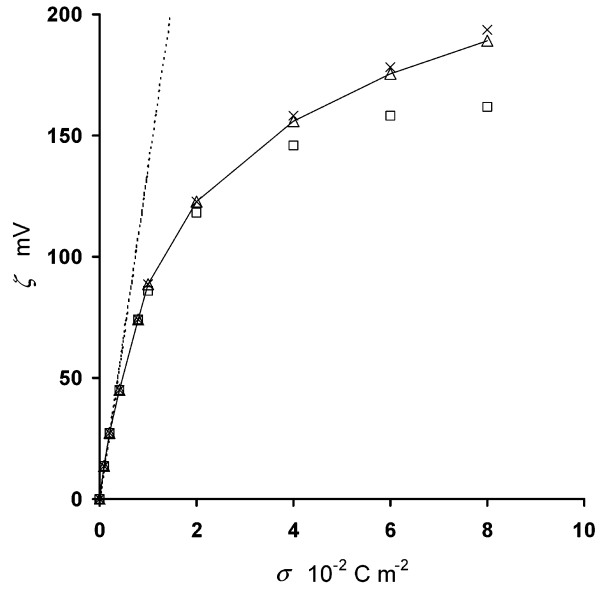


Figure 3. ζ-Potential as a function of the surface charge density. Simulated results (×) are compared with the results of Attard, who studied several models: LPB, - -; PB, ×; HNC, □.

bulk concentrations are imposed for the ion-flux equations. The connecting boundaries between the charged surface and its opposite boundary are insulators.

The two ions have a bulk concentration of 1.0 mol $m^{-3}$, the diffusion coefficients are equal to $1.0 \times 10^{-9}$ $m^2$ $s^{-1}$, and the temperature is 300 K. A structured grid with a minimal element dimension of typical 1% of $\lambda$ that grows out with a factor 1.5 normal to the charged surface is used to compute the potential and concentration fields. Recently, Attard and al.[19] studied different models for the HDL in the same circumstances. They calculated and measured the charge density $\sigma$ on the surface as a function of the ζ potential. Among others, the LPB, the exact PB, and the hypernetted chain (HNC) theory were applied, and it was found that the HNC results are the closest to measurements. Figure 3 shows the computed ζ potential, as compared to the analytical values,[19] for several values of the surface charge density $\sigma$. The present model is inherently characterized by the exact PB equation ,and therefore, the results are very close to these of Attard. The small deviations for higher charge densities could be improved using more elements for the discretization.

**Potential and Velocity Distribution.** The second case is a comparison between computed and analytical potential and velocity distributions of a binary electrolyte in a rectangular channel having a height of 0.1 $\mu$m and a length of 100 $\mu$m. These rather small dimensions are chosen in view of the validation with analytical results. For all calculations, a grid was used containing 33 400 elements and 17 400 nodes. This grid was certainly not optimized toward computational speed, but ensures numerical accuracy in all cases that were calculated. The dimensions of the channel and the imposed boundary conditions are shown in Figure 4. The applied potential difference over the length is 1.0 V, yielding an electric field of 10 kV $m^{-1}$. At the inlet on the left, 0 potential, 0 pressure, and the bulk concentrations are imposed. At the charged surfaces, the velocity and the concentration fluxes are put equal to 0, whereas the gradient of the potential equals the imposed value of $-\sigma/\epsilon$. At the outlet on the right, 0 pressure and bulk concentrations are imposed, and the outlet potential is 1.0 V. Figure 5 shows the calculated concentration distributions in mol $m^{-3}$ normal to the insulating walls taken at the center of the channel ($x = l/2$) for two different values of the bulk concentrations $c_0$, 1 and 10 mol $m^{-3}$. The results are calculated for a charge density of $7.25 \times 10^{-5}$ C $m^{-2}$.

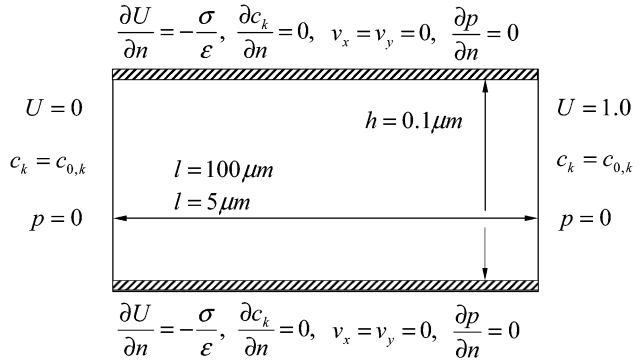


Figure 4. Dimensions and boundary conditions for the computation of a channel flow.

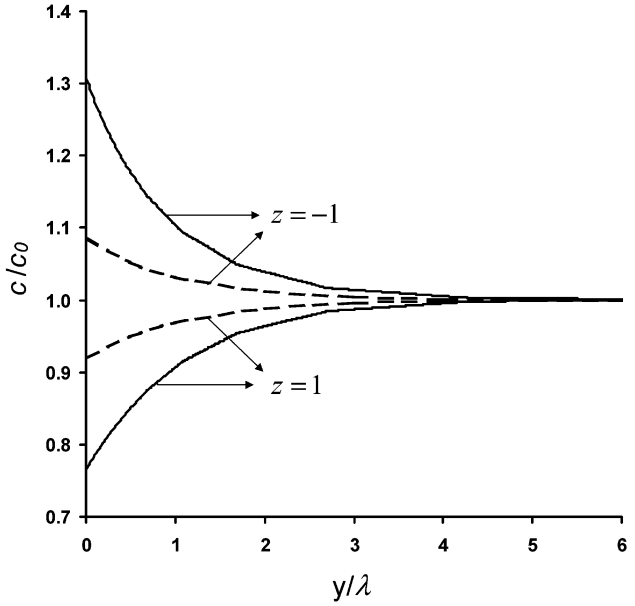


Figure 5. Ion-concentration distribution normal to the surface in the central cross-section of a channel in relation to the dimensionless distance $y/\lambda$. The results are calculated for a total charge of $7.25 \times 10^{-5}$ C $m^{-2}$ and bulk concentrations $c_0 = 1$ (—) and 10 (– –) mol $m^{-3}$.

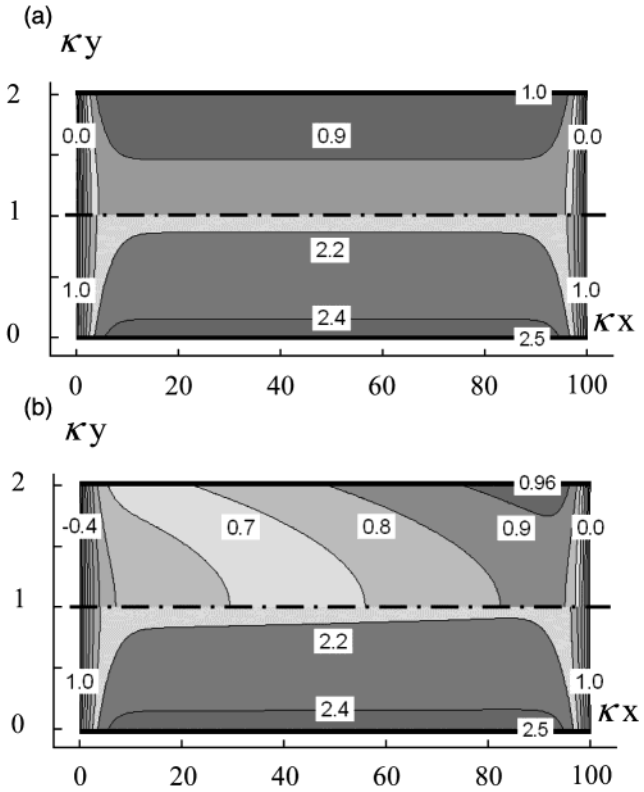


Figure 6. Scaled isopotential lines (upper half) and isoconcentration lines (lower half) are shown in a very small channel. The $\zeta$ potential of 25.5 mV and the diffuse layer build up gradually. (a) Without external electrical field, (b) in the presence of an imposed electric field of 2000 V m$^{-1}$.

So far maybe of less practical use, it is interesting to consider also the influence of the channel entrance. Because the channel is at 0 volts and the charge density is applied along the wall, the diffuse layer and the $\zeta$ potential are built up gradually. This is shown in Figure 6a and b, where, respectively, no external electric field and a field of 2000 V m$^{-1}$ is applied. Equipotential lines and concentration field vary continuously. Similar results can easily be obtained for any geometrical configuration.

In Figure 7, the scaled potential distributions (also scaled velocity profiles) are plotted in full and dotted lines along the central cross section of the channel for $c_0$ equal to 0.00924, 0.0369, 0.148, and 0.591 mol m$^{-3}$. The computed values are compared with the results of Burgreen and Nakache,[6] who derived in 1964 an analytical expression for an infinitely long channel. In all cases, the computed $\zeta$ potential equals 0.02557 V, and thus, $\alpha = F\zeta/RT = 1.0$ C V J$^{-1}$, or 0.1023V for $\alpha = 4.0$ C V J$^{-1}$. The quantity $\kappa h = h/\lambda$ appearing in the abscissa, is the height of the channel expressed in multiples of the Debye length $\lambda$, defined as follows:

$$\kappa = \frac{1}{\lambda} = \sqrt{\frac{\sum_k z_k^2 F^2 c_k}{\epsilon RT}} \qquad (12)$$

The computed results match very well with the theoretical results, confirming the potentialities of the DSM with the Poisson−Boltzmann equation as an accurate model for the computation of potential and concentration distributions in micrometer or submicrometer features.

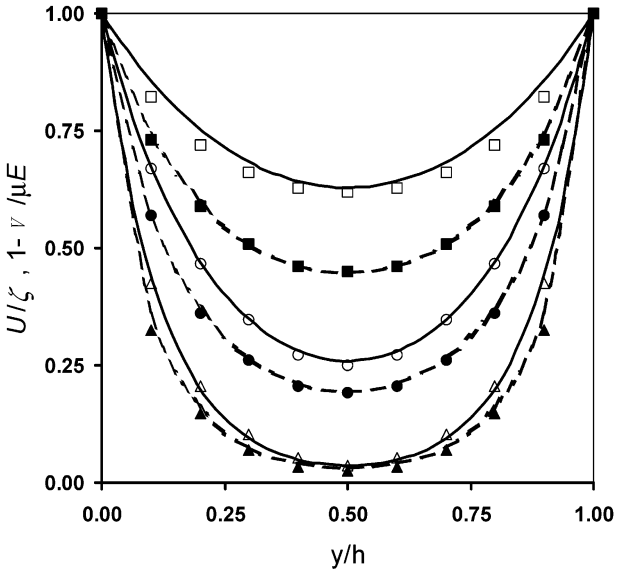


Figure 7. Potential distribution and velocity profile plotted along the central cross section of the channel. Comparison between computed values and values obtained by Burgreen and Nakache. For $\alpha = 1$ and $\zeta$ potential = 0.02557 V, the computed values are solid lines: □, $\kappa h = 2$; ○, $\kappa h = 4$; △, $\kappa h = 8$. For $\alpha = 4$ and $\zeta$ potential = 0.1023 V, computed values are broken lines: ■, $\kappa h = 2$; ●, $\kappa h = 4$; ▲, $\kappa h = 8$.

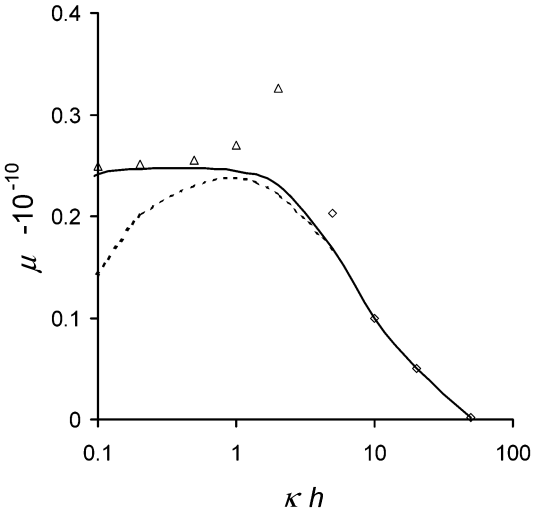


Figure 8. Maximal values of the mobility as a function of the scaled channel height. Analytical expressions for an infinitely long channel; expression valid for large $\kappa h$ (◇) and for small $\kappa h$ (△). Numerical results: channel length of 100 $\mu$m (solid line) and 5 $\mu$m (broken line). The charge density is equal to $10^{-4}$ C m$^{-2}$.

**Mobility.** One can further consider the influence of the channel height on the velocity and, hence, the mobility, which is defined as the velocity divided by the electric field. Because the velocity varies along the cross section, all results will be given for the maximum mobility, which is reached at $y = h/2$. So the calculated mobility is obtained using the computed maximum axial velocity, the length of the channel, and the potential difference applied between inlet and outlet. Thus, in Figure 8, calculated mobilities are shown for different values of $\kappa h$ (obtained by

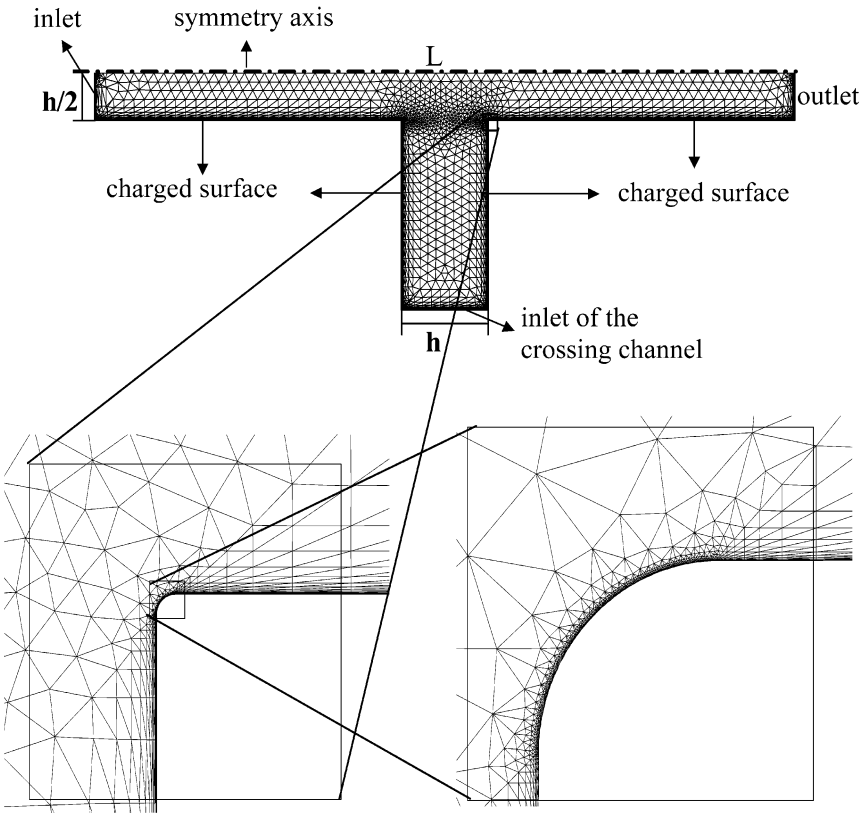


Figure 9. Geometry and details of the grid used for the computation of the EOF in a cross channel.

changing bulk concentrations) and compared with analytical expressions.

For large values of $\kappa h$, the mobility $\mu$ was derived by, for example, Probstein[11] and equals

$$\mu = \frac{v}{E} = -\frac{\epsilon\zeta}{\mu_h}(1 - e^{-(h-r)/\lambda}) \qquad (13)$$

with $r$ the normal distance from the charged surface.

Notice that for thin diffuse layers, $\kappa h > 10$, eq 13 equals the Helmholtz−Smoluchowski formulation for the mobility. For values of $\kappa h$ smaller than 6, eq 13 is no longer valid. The two HDLs start overlapping such that the net amount of electrical charge between the two opposite surfaces becomes smaller. A limiting case is found when the ion concentrations over the width of the channel become constant ($\kappa h < 1$). The analytical solution of the axial velocity, $v$, is then obtained by integrating eq 6 while neglecting convection and pressure. Using eq 10 for the concentration field yields finally

$$v = -\frac{h^2 E}{4\mu_h} zFc_0 \sinh\left(\frac{zF\zeta}{RT}\right) \qquad (14)$$

It can be observed in Figure 8 that the presented numerical approach is valid for any value of $\kappa h$ and that a continuous transition of the mobility is obtained. When one considers a long channel (100 $\mu$m, full line) for large heights with respect to Debye length, the results correspond to the HS values, and for small heights, eq 14 is valid.

These results not only solve the question of the transition region but also the effect of a finite channel length is considered. Indeed, for very small values of $\kappa h$, a deviation is again observed. In the calculations, the transitions at inlet and outlet influence the overall velocity field. This is clearly demonstrated when a very short channel length of 5 $\mu$m is taken for which the dotted line represents the corresponding maximum mobility. Edge effects become dominant for small heights, and in fact, the $\zeta$ potential is changing continuously along the wall. A situation similar to the one presented in Figure 6 occurs.

## STUDY OF A CROSS CHANNEL

Patankar and Hu[13] made one of the interesting contributions about EOF simulations. They used a cross-channel geometry to test their numerical code. Their model uses two electrical potential equations combined with the LPB approximation such that the charge distribution is not directly coupled with the Lorentz force. The challenge here is to show that simulations based on the full MIM model are possible and that simulated results are at least qualitatively in agreement (quantitative comparison appeared difficult). The purpose of a cross channel is to inject a specific amount of liquid from a side reservoir, via the cross channel, in a main channel where it will be transported and eventually analyzed. To control this injection mechanism, the potentials at the inlets and outlets are changed.

In Figure 9, half of a cross channel with symmetry axis is shown. The inlet is on the left, the outlet on the right. The cross channel is situated in the middle at the bottom. The symmetry

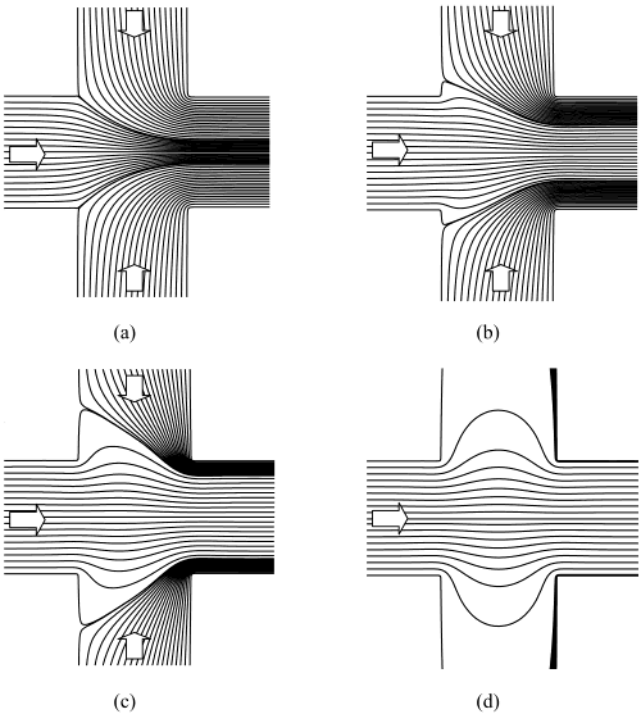


Figure 10. Streamlines in the cross channel. The imposed potential at the inlet of the main channel is 0, and the at the outlet, is 0.01 V. The imposed potential at the inlet of the crossing channel equals 0 V (a), 0.0025 V (b), 0.004 V (c) and 0.005 V (d). The arrows indicate the direction of the fluid movement. The charge density on the charged surfaces is $-1.35 \times 10^{-4}$ C m$^{-2}$.

axis is positioned at the top. By changing the potential at the inlet, the outlet, and the inlet of the cross channel, one can control the flow coming from or going to the cross channel. Figure 9 also shows a detailed plot of the intersection of the cross channel with the main channel. The grid has 6694 points and 12 686 elements and was made with the hybrid grid generator.[23] On the boundaries, a structured layer is present in order to capture the concentration, potential, and pressure gradients near the charged surfaces. A constant charge is imposed on each charged surface. The potential at the inlet $U_{in}$ and the outlet $U_{out}$ are imposed and EOF occurs. Gradually, the potential at the inlet of the cross channel $U_{cr}$ is increased from $U_{in}$ to $(U_{out} + U_{in})/2$. Figure 10 shows the corresponding streamlines.

## CONCLUSIONS

A general applicable two-dimensional multi-ion model to calculate electroosmotic flow based on the dilute solution model and the Navier−Stokes equations has been proposed. The boundary conditions appear more "natural", because on surfaces, the local charge density is imposed, not the $\zeta$ potential. Therefore, the rather artificial separation into a solution potential and a $\zeta$ potential is also avoided. This approach enhances physical relevance, since in reality, the $\zeta$ potential is not known and depends on the local concentration distribution of the ionized species. The proposed model is able to predict the potential distribution and mobilities in multi-ion systems and can be applied to any geometry. Local effects on the scale of the Debye length can be studied in detail. This allows modeling of nanoscale applications.

The simulated results for potential distributions and mobilities match with analytical solutions that are available only for binary electrolytes. The model has been used to predict the flow patterns in a cross channel during injection.

These results indicate that the proposed numerical model has all the potentialities to describe multi-ion electroosmosis accurately.

## GLOSSARY

| | |
|---|---|
| $c$ | ion concentration, mol m$^{-3}$ |
| $c_0$ | bulk ion concentration, mol m$^{-3}$ |
| $D$ | molecular diffusion, m$^2$ s$^{-1}$ |
| $E$ | electric field, V m$^{-1}$ |
| $F$ | Faraday constant, 96485 C mol$^{-1}$ |
| $h$ | height of the rectangular channel, m |
| $J$ | current density, A m$^{-2}$ |
| $l$ | length of the rectangular channel, m |
| $N$ | ion flux, mol m$^{-2}$ |
| $p$ | pressure, Pa |
| $r$ | radius, m |
| $R$ | universal gas constant, 8.31 J mol$^{-1}$ K$^{-1}$ |
| $t$ | time, s |
| $T$ | temperature, K |
| $U$ | electric potential, V |
| $U_{out}$ | applied potential at the outlet, V |
| $U_{in}$ | applied potential at the inlet, V |
| $U_{cr}$ | applied potential at the inlet of the cross channel, V |
| $v$ | velocity, m s$^{-1}$ |
| $z$ | ionic valence |

Greek symbols

| | |
|---|---|
| $\alpha$ | $F\zeta/RT$, C V J$^{-1}$ |
| $\epsilon$ | permittivity, C V$^{-1}$ m$^{-1}$ |
| $\lambda$ | Debye length, m |
| $\kappa$ | inverse of Debye length, m$^{-1}$ |
| $\mu$ | mobility, m$^2$ V$^{-1}$ s$^{-1}$ |
| $\mu_h$ | hydraulic diffusion coefficient, m$^2$ s$^{-1}$ |
| $\rho$ | density, kg m$^{-3}$ |
| $\rho_e$ | charge density, C m$^{-3}$ |
| $\sigma$ | surface charge density, C m$^{-2}$ |
| $\zeta$ | zeta potential, V |

Matrix Convention

$\bar{N} = \sum_{i=1}^{\dim} N_i \overline{1_i}$

Abbreviations

| | |
|---|---|
| DSM | dilute solution model |
| EOF | electroosmotic flow |
| FE | finite elements |
| HDL | Helmholtz double layer |

| | |
|---|---|
| HNC | hypernetted chain |
| HS | Helmholtz−Smoluchowski |
| LPB | linear Poisson−Boltzmann |
| MEMS | microelectromechanical systems |
| MIM | multi-ion model |
| $\mu$TAS | micrototal analysis systems |
| NS | Navier−Stokes |
| PB | Poisson−Boltzmann |

## ACKNOWLEDGMENT

This work was funded by the European Commission Desiner project BE-97-4761 and by the Vrije Universiteit Brussel G.O.A. project no. 11.

Received for review March 4, 2002. Accepted July 20, 2002.

AC025609S